Nonequilibrium Behavior of Current Carrying Supersonic Rare Gas Flow

H. Frey*
Insitut für Plasmaforschung der Universität Stuttgart, Stuggart, Germany

Nonequilibrium ionization in a rare gas mixture containing a readily ionizable particle species can be used to replace rare gas-alkali mixtures. A rare gas plasma, consisting of neon and 2% xenon is produced in a gasdynamic-diaphragm shock tube with pressures between 220 and 840 torr and gas temperatures between 3700 and 5800 K. The electrical conductivity is determined from measurements of current density and potential profiles. It is also directly measured by the induction method. The theoretical treatment is based on a multicomponent theory in which the individual particle species in the plasma are treated separately and the interactions between the components are expressed by production and energy transfer rates in the conservation equations. The agreement between theoretical model results and experimental electrical conductivity measurements is good.

Introduction

WHEN an electric current is passed through a partially or fully ionized gas, it is primarily the electrons which gain energy from the resulting electric field. They then try to transfer this energy to the heavier particles (atoms and ions) as a result of collisions. If inelastic collisions predominate, good energy contact between the electrons and atoms or ions is established. Consequently, with a sufficiently high collision frequency, there is approximate temperature equilibrium between the light electron gas and the comparatively heavy atom or ion gas. If, on the other hand, the collisions are purely elastic, the energy transfer shows a decisive dependence on the mass ration m_e/m_A.

A large difference in mass weakens the energy coupling, can become, and this may cause a strong elevation of the electron temperature above the gas temperature. This effect is observed in the glow discharge. This nonequilibrium effect is of special significance in connection with the development of magnetohydro-dynamic generators, which are to be used for converting the thermal energy in nuclear reactors into electric energy. Since the output temperatures of the rare gas used for cooling the reactor are too low to produce sufficient ionization, it was proposed by Kerrebrock[1] that the cooling gas be seeded with a small amount of a readily ionizable material such as Cs or K.

After entering the generator, the few thermally produced electrons gain energy in the effective electric field of the generator. Only a small fraction of this energy can be transferred to the rare gas atoms, since the electron-atom collisional process is purely elastic due to the large first excitation energy level of the rare gas atoms. Energy equilibration thereby requires a large number of elastic collisions. The temperature of the electrons will, thus, rise above the gas temperature. This temperature rise will increase their chance to ionize the alkali-atoms. The electron density n_e, and hence the conductivity δ, which in this region of ionization depends directly on n_e, will increase significantly.

The nonequilibrium effect is usually studied in rare gas alkali mixtures,[1-3] which are awkward to handle. It seems easier, however, to use a helium-xenon or a neon-xenon mixture, even if a higher temperature is required. This choice was suggested by the convenience with which helium-xenon or neon-xenon mixtures could be studied, because the first excitation level of xenon (8.315 eV) is some 11.499 eV below that of helium (19.814 eV) and 8.3 eV below that of neon (16.615 eV).

If a small quantity of xenon is admitted to a helium or neon flow and if it is assured that the gas temperature prior to entry into the electric field is just high enough to start ionization of the xenon ($\sim$3000 K), the few thermally produced electrons can transfer their energy to the numerically superior helium or neon atoms only in the form of elastic collisions, as in an argon-potassium mixture. Here, too, the electron temperature has to rise, thus leading to higher ionization of the xenon.

These effects can be investigated to particular advantage with a shock tube in which hydrogen is used as driver gas and helium or neon containing a small quantity of xenon as work gas. Neon was chosen as background gas. It is easier to heat than helium, owing to the low sound velocity in a shock tube. If electrodes are mounted on the tube walls, the nonequilibrium effect can be observed behind the shock wave.

With the appropriate initial pressure ratio it is possible to vary slightly the Mach number and, hence, the temperature behind the shock wave, while the current density for producing the nonequilibrium condition can be set quite independently by applying the appropriate voltage. In principle, such investigations could also be made directly in electric discharges. In that case, the gas temperature could also be determined by discharge current causing the nonequilibrium condition. Variation of the two quantities independently of one another would not be possible.

The basis for the theoretical treatment of the expected changes of state of the plasma is provided by the conservation laws for mass, momentum, and energy of the individual components of the plasma. The components of the work gas are assumed to be neon as background gas, xenon as seed gas, xenon ions and electrons. The interaction processes between the components are expressed in terms of particle production and energy transfer rates. The ionization process is determined by using a two-step model for the reacting plasma component (xenon), the excitation rate of the first level rather than ionization rate being the dominant factor.

Experimental Investigations

A schematic plan of the discharge zone in the diaphragm shock tube[4] used in this experiment is depicted in Fig. 1. All sections of the tube were sealed with O-rings, which were adequate to permit evacuation to pressure levels of approximately 10^{-5} torr. The driver section, consisting of a 1.7 m length of the whole 12-m tubing, permitted driver pressures up to 100 atm to be attained. The initial driven gas pressure was adjustable, within an error of less than 0.1 torr, to any pressure in the range $\sim$1-20 torr. Experiments were con-

Received July 10, 1975; revision received Oct. 31, 1975.
Index category: Plasma Dynamics and MHD.

*Research Engineer. Now at Leybold Heraeus Gmbh und Co., Hanau, BRD.

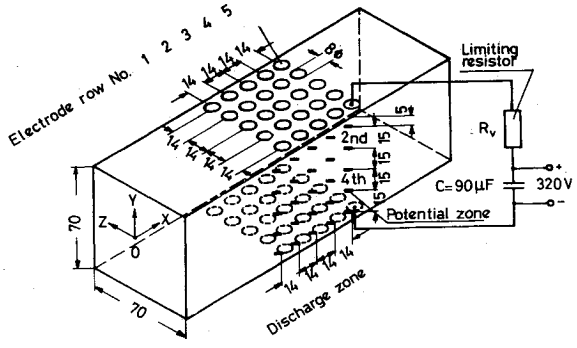

Fig. 1 Arrangement of electrode and potential probes, with most important dimensions.

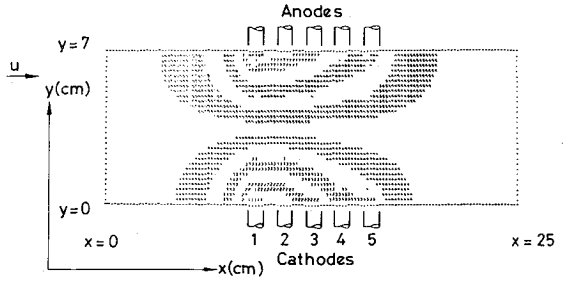

Fig. 2 Experimentally determined potential distribution; shock Mach number $M_s = 7$, gas pressure $p = 488$ torr, total current in five electrode rows $I_g = 252$ A.

ducted with driving pressures in a limited range of 4 to around 16 torr.

Depending on the experimental conditions, there is in the discharge zone a current of 4-10 A per electrode pair. The discharge currents can be set by using limited resistors. The shock front velocity and the pressure were measured with piezoelectric pressure probes.

The electrical conductivity δ in the center of the channel can be calculated from the potential distribution and the electrode currents. The electrode currents were measured with dc current probes, the potential distribution with potential probes. The measured potential distribution for a typical test is shown in Fig. 2.

The oscillograms in Fig. 3 show the time development of the voltage between the second and fourth potential probes and that of the current in the individual rows of electrodes. The potential probe signals show that the collision front is characterized at the beginning by a very fast rise. The assured ignition high-pressure gas discharge occurs because a significant number of thermally produced charged particles is provided by the plasma flow, and because the charge balance is positive. The stabilization of the discharge after breakdown results from the attainment of equilibrium between the increase and loss of charged particles. If the time behavior of the voltage in the rows of the electrodes is considered, it can be seen that the field strength along the channel axis remains constant in time on the average from about 100 μsec after breakdown until arrival of the contact zone at the test location. Within this time difference (~ 250 μsec) there is a stationary and spatially fixed distribution of the flow rate and state variables behind the shock front. The theoretical investigation refers to this region.

On arrival of the contact zone, and hence of the electrically nonconducting driver gas, at the test site the discharge undergoes a change of shape. This is revealed by the time variation of the potential probe and current probe signals. The current probe signals immediately drop, while the signal of the potential probes, having reached a peak, slowly return to zero. This indicates that the charged particles which are transported through the boundary layer to regions behind the contact zone cause, for some tens of microseconds, a

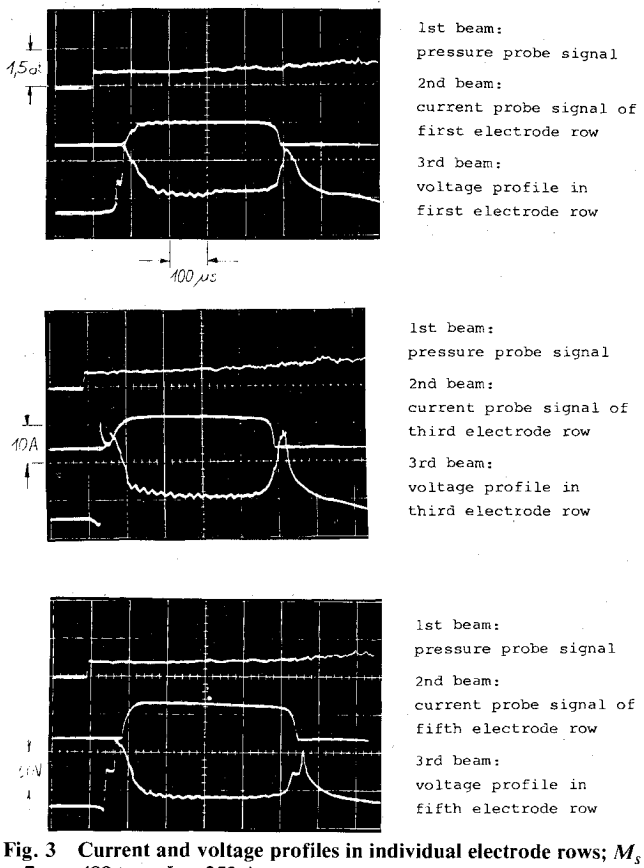

Fig. 3 Current and voltage profiles in individual electrode rows; $M_s = 7$, $p = 488$ torr, $I_g = 252$ A.

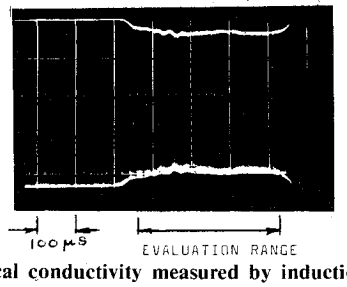

Fig. 4 Electrical conductivity measured by induction method; $M_s = 7$, $p = 488$ torr, $I_g = 252$ A.

discharge with very much lower current density ($\sim 10^{-4}$Acm^{-2}) than the shock wave (~ 4 Acm^{-2}). The irregularity of this peak could be caused by the turbulent mixing of the cold driver gas and the hot test gas behind the contact front.

The electrical conductivity δ outside the discharge zone was measured by the induction method.[5] Argon or argon-xenon shock waves whose conductivity is known[6] were used as calibration standards. To avoid, if possible, disturbances that might be due to the discharge (e.g., magnetic fields induced by the discharge currents), the measurement was made 25 cm below the discharge zone. The fluctuations superposed on the envelope (Fig. 4) of the oscillation amplitude of the test frequency are due to resistance fluctuations in the shock-heated gas.

Theoretical Investigations

The theoretical investigations are based on the conservation laws for mass, momentum, and energy each of the individual components of the plasma.[7] It was assumed that the components comprised neon as background gas, which is not ionized or excited in the temperature range considered (3600-5800 K), xenon as readily ionized seed gas, xenon ions and electrons. The calculation was mathematically simplified by

assuming one-dimensionality, which means all flow and state variables have constant spatial profiles perpendicular to the flow direction.

Estimates show[8] that in the parameter range investigated (gas temperature $T_G = 3600$-5800 K, electron temperature $T_e = 3600$-$18{,}000$ K, electron density $n_e = 10^6$-10^{14} cm^{-3}, density of the heavy particles $n_s = 4\times10^{17}$-4×10^{18} cm^{-3}) the radiation losses of the plasma are negligible. Dissipative terms in the conservation equations for the heavy plasma components which describe viscosity and thermal conduction are also ignored because the velocity and gas temperature gradients are only small. This reasoning allows the assumption in the calculation that all heavy particles have equal velocities as well as equal temperatures.

Assuming quasineutrality and the simplifications mentioned, it is possible to formulate the following system of equations in a shock-fixed coordinate system.

Equations of continuity

$$(d/dx)\,(n_e u) = \dot{n}_e \tag{1}$$

$$(d/dx)\,[(n_N + n_X + n_i)u] = 0 \tag{2}$$

where n = particle density, u = flow velocity, n_r = production rate, r = component, N = neon, i = ions, X = xenon, e = electrons, s = heavy particles (atoms, ions).

The production rate $\dot{n}_e$, obeying the relations

$$\dot{n}_e = \dot{n}_i = -\dot{n}_e \tag{3}$$

expresses the number of electrons which are newly produced per unit time and space by reactions. It is given by

$$\dot{n}_e = n_e n_X I_{eX} + n_X n_N I_{Nx} + n_X n_X I_{Xx} - n_N n_e n_i R_{NX} - n_X n_e n_i R_{XX} - n_e^3 R_{eX} \tag{4}$$

where I_{rX} = excitation rate coefficient and R_{rX} = recombination rate.

The collisional excitation rate constants I_{rx} are obtained from Ref. 9 and the three body collision recombination constants R_{rx} are used from Ref. 10.

The ionization process is studied by using a two-step model for the reacting xenon in which the excitation energy and not the ionization energy is the governing factor.[11]

Momentum equation

$$(m_N n_N + m_X n_X + m_i n_i)\,u\frac{du}{dx} - (n_N + n_X + n_i)\,\frac{kT_s}{u}\,\frac{du}{dx} + (n_N + n_i + n_X)\,k\frac{dT_s}{dx} = 0 \tag{5}$$

where k = Boltzmann constant and m = atomic mass.

Energy equations

$$\frac{d}{dx}\left\{\left[\frac{5}{2}(n_N + n_X + n_i)\,k\,T_s + \tfrac{1}{2}m_N n_N u^2 + \tfrac{1}{2}m_i n_i u^2\right]u\right\} = \bar{Q}_s \tag{6}$$

$$\frac{d}{dx}\left[\left(\frac{5}{2}n_e k\,T_e + \tfrac{1}{2}m_e n_e u^2\right)u\right] = \bar{Q}_e \tag{7}$$

where $\bar{Q}_r$ = energy source term

The energy source term $\bar{Q}_r$ on the right-hand side of the two equations describes the energy gain or loss due to elastic and inelastic collisions of the plasma components per unit volume and time with one another. $\bar{Q}_e$ is given by

$$\bar{Q}_e = \frac{j_e^2}{\delta} - 3m_e n_e k(T_e - T_s)\left(\frac{8k\,T_e}{\pi m_e}\right)^{1/2}\left(\frac{n_N Q_{eN}}{m_N} + \frac{n_X Q_{eX}}{m_X} + \frac{n_e Q_{ei}}{m_i}\right) - \left(n_e n_X I_{eX} - n_e^3 R_{eX}\right)\left(\frac{3}{2}k\,T_e + E_{Ix}\right) \tag{8}$$

where E_{Ix} = ionization energy from xenon, and j = current density.

The first term on the right-hand side j_e^2/δ represents the energy gain of the electrons in the electric field. Owing to the high mobility of the electrons (their drift velocities are about 400 times as large as those of ions) the current is transported almost exclusively by electrons (i.e., $j_e = j$). The momentum transfer cross sections Q_{eN}, Q_{eX}, and Q_{ei} are taken from Ref. 12.

The third term gives the energy transfer rate to the free electrons by electron-atom and electron-ion-electron inelastic collisions, where $(3/2)k \cdot T_e$ is the energy which is necessary to heat a newly produced electron to the local electron temperature. Finally, the transfer rate of energy to the free electrons can be written as

$$\bar{Q}_s = 3m_e n_e k(T_e - T_s)\left(\frac{8k\,T_e}{\pi m_e}\right)^{1/2}\left(\frac{n_N Q_{eN}}{m_N} + \frac{n_X Q_{eX}}{m_X} + \frac{n_e Q_{ei}}{m_i}\right) - (n_X n_N I_{NX} + n_X n_X I_{XX} - n_N n_e n_i R_{NX} - n_X n_e n_i R_{XX})\left(\frac{3}{2}k\,T_e + E_{Ix}\right) \tag{9}$$

with the first term giving the contributions from electron-atom and electron-ion elastic collisions, the second term those from atom-atom and atom-ion inelastic collisions.

The initial values after the shock front needed for the calculation were determined by means of the Rankine-Hugoniot relations and the Sahaequation using the given shock Mach numbers M_s (ratio of the shock front velocity to the sound velocity in the static working gas). The values reached experimentally were given by the current density j. Both the numerical solution of the Rankine-Hugoniot relations and Sahaequation and the integration of Eqs. (1-7) were performed using the University of Stuttgart CDC 6600 computer system.

Comparison of Theory and Experiment

The distribution of the electrical conductivity δ, which is obtained from the nonequilibrium calculations, is shown in Fig. 5 for three examples. Measured conductivity values have been plotted along with the theoretical values. Inside the discharge zone, δ was determined from the potential distribution and current density, outside by the induction method. The deviations of the measured conductivity values by the induction method, outside the electrode zone, are below 15%.

The agreement between the calculated and measured values is surprising, considering the simplifying assumptions of the one-dimensional calculation. The different directions of the deviations between the theoretical and experimental valus inside and outside the discharge zone reveal the difference between the two measuring methods for determining δ.

The value of the conductivity obtained using the induction method is a mean effective value in the plasma volume permeated by the alternating magnetic field. Due to the fact that the charged particle density, and hence the conductivity, in the electrode boundary layers is much higher than in the center of the channel and the fact that the simplified calculation model is valid only along the channel axis, the experimental results are higher than the theoretical ones. In addition, at the low

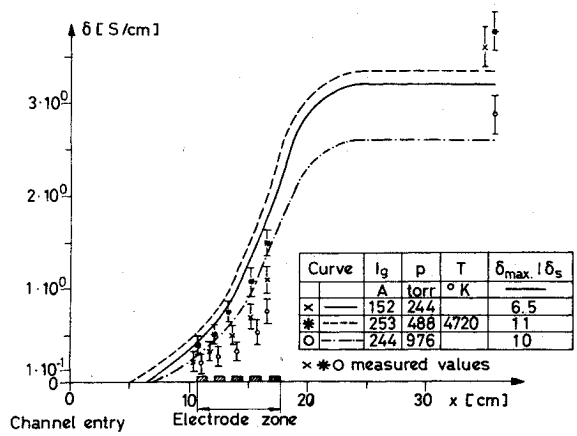

Fig. 5 Theoretical and experimental distribution of electrical conductivity δ; $M_s = 7$.

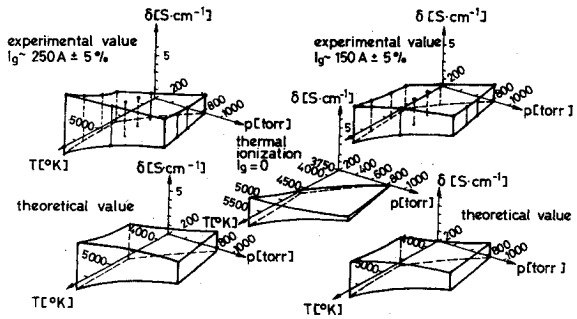

Fig. 6 Conductivity values in theoretically and experimentally investigated parameter range.

values of electron density prevailing in the discharge region, impurities, e.g., in the form of metal vapor, play a significant role, since their ionization energy is smaller relative to that of xenon ($Fe = 7.9$ *eV*, Cu = 7.39 *eV*, Al = 5.98 *eV*, etc). The metal vapor is unavoidable owing to the slight electron burnup. In the discharge volume, on the other hand, where the conductivity is determined from the potential distribution and the current density, the values determined experimentally are lower than those calculated. Apart from the uncertainty involved in the cross-sections, the calculations also include several other simplifying assumptions, such as complete homogeneity of the plasma on entry of the flow into the discharge region, which are not wholly realized in the experiment.

To gain an overall picture of the conductivity due to the nonequilibrium ionization, the theoretically calculated results and those measured by the induction method for all the parameters experimentally investigated in this study have been compiled in Fig. 6. The calculated values of the conductivity for the case of thermal ionization only ($I_g = 0$) are also presented in Fig. 6. Under the experimental conditions $p = 765$ torr and $T_a = 3750$ K the nonequilibrium ionization conductivity exceeds the thermal-ionization conductivity by a factor of 350.

Five rows of electrodes were always used to generate the electric field. The total current I_g was either 150 A or 250 A, with a deviation of 5%. In the entire parameter range the experimental results are greater than the theoretical values. The deviations are between 20 and 60%.

Conclusions

Nonequilibrium ionization by applied electric field for the purpose of improving the electrical conductivity was investigated experimentally and theoretically in a neon supersonic flow containing 2% neon. A simple system of equations has been developed to calculate the enhancement of the electrical conductivity δ as a function of the gas pressure, the gas velocity, and the discharge current. Reasonable agreement between theory and experiment has been established. In the best case an increase by a factor of 350 relative to δ in the case of thermal equilibrium ionization was observed at a gas pressure of 840 torr and a gas temperature of 3750 K.

In connection with the continuation of nuclear powerplant development with gas-cooled high-temperature reactors to attain higher working temperatures, it should be possible to use MHD generators. As nuclear fuel costs are relatively low, the price for power strongly depends on investment costs, and so the simplest design should be sought.

A simple possible solution might be to incorporate an MHD generator backed by a gas turbine in the closed primary circuit. In this type of powerplant the work gas passes directly through the reactor. In this case only rare gases are suitable as the work gas, since reaction with the fuel elements in the reactor has to be avoided. If C_s of K is used as seed material it has, therefore, to be removed from the work gas before entry into the reactor. For this reason it is interesting to replace the alkali with another seed material.

The fairly good agreement between theoretical and experimental conductivity values could open the possibility of using rare gas mixtures as the work gas in high-temperature reactors with a coupled MHD-generator. The simulation of nonequilibrium ionization for increasing δ can be done with simple one-dimensional calculation models.

References

[1] Kerrebrock, J. L., "Magnetohydrodynamic Generators with Nonequilibrium Ionization," *AIAA Journal*, Vol. 3, April 1965, pp. 591-601.

[2] Riedmüller, W., "Messungen der Elektronentemperatur in einem Argon Kalium Plasma," Rept. IPP 3/31, 1965, Max-Planck-Institut für Plasmapysik, Garching bei München, BRD.

[3] Schwenn, R., Brederlow, G., and Salvat, M., "Electrical Conductivity of an Argon-Potassium Plasma at Low Current Densities as Function of the Gas Temperature," *Plasma Physics*, Vol. 10, 1968, pp. 1077.

[4] Nett, H., "Überlegungen zum Bau eines Membran-StoB-Wellenrohres für Plasmaexperimente und erste Messungen," Rept. IPP 3/43, 1966, Max-Planck-Institut für Plassmaphysik, Garching bei München, BRD.

[5] Rapp, H. and Moser, F., "Ortskurven der Impedanz und Admittanz eines Solenoids mit homogenen leitfähigem Kern," Rept. IPF 1/27, 1968, Institut für Plasmaforschung der Universität Stuttgart, BRD.

[6] Holzhauer, E., "Experimentelle und theoretische Untersuchungen magnetohydrodynamischen Strömungsvorgänge mit transversalem Magnetfeld im StoBwellenrohr," Rept. IPF 73/5, 1973, Institut für Plasmaforschung der Universität Stuttgart, BRD.

[7] Eichert, K., "Die eindimensionale Magneto-Plasmaströmung mit Nichtgleichgewichtsionisation- und Anregung," Rept. IPF 71/2, 1971, Institut für Plasmaforschung der Universität Stuttgart, BRD.

[8] Schrade, H., Bez, W., Höcker, K. H., and Kaeppler, H. J., "Zur Theorie der Ohmischen Heizung vollionisierter Plasmen," *Zeitschrift fur Naturforschung*, Vol. 15a, Heft 2, 1960, pp. 155-168.

[9] Chapmann, S. and Cowling, T. G., *Theory of Nonuniform Gases*, Cambridge University Press, Cambridge, England, 1970.

[10] Morgan, E. J. and Morrison R. D., "Ionization-Rates Behind Shock Waves in Argon," *The Physics of Fluids*, Vol. 8, 1965, pp. 1608.

[11] Harwell, K. E. and Jahn, R. G., "Initial Ionization-Rates in Shock-Heated Argon, Krypton and Xenon," *The Physics of Fluids*, Vol. 7, 1964, pp. 214.

[12] Brown, S. C., *Basic Data of Plasma Physics*, M.I.T. Press, Cambridge, Mass.

[13] Kelley, A. J., "Atom-Atom-Ionization Cross Section of the Noble-Gases Argon, Krypton, Xenon," *Journal of Chemical Physics*, Vol. 45, 1966.

[14] Frey, H., "Experimentelle und theoretische Untersuchung der überthermischen Leitfähigkeit einer Überschallströmung bei Stromdurchgang," Rept. IPF 74/9, 1974, Institut für Plasmaforschung der Universität Stuttgart, BRD.